

Cyclic Mechanical Properties of Q960 High Strength Steel Considering Salt Spray Corrosion

Sikai Liu¹, Shidong Nie^{1,2,*}, Zhenye Chen³, Cheng Ma³, and Jin Pan³

¹School of Civil Engineering, Chongqing University, Shapingba District, Chongqing, China

²Key Laboratory of New Technology for Construction of Cities in Mountain Area (Chongqing University), Ministry of Education, Shapingba District, Chongqing, China

³User Technology Center of Materials Technology Research Institute of HBIS, Shijiazhuang, China
Email: 807511857@qq.com (S.K.L.); nieshidong@cqu.edu.cn (S.D.N.); chenzy@hbisco.com (Z.Y.C.); acheng01@hbisco.com (C.M.); panjin@hbisco.com (J.P.)

*Corresponding author

Abstract—In order to study the corrosion resistance and cyclic mechanical properties of the new domestic Q960 high-strength steel, this paper conducted cyclic loading tests on 7 Q960 high-strength steel cyclic material properties specimens under 7 different loading regimes, and 10 Q960 high-strength steel cyclic material properties specimens were subjected to different degrees of salt spray corrosion tests and cyclic loading tests after corrosion, and the skeleton curves and energy dissipation coefficients of the steel before and after corrosion were extracted, and the cyclic mechanical properties of the steel before and after corrosion were evaluated. The cyclic mechanical properties of the steel before and after corrosion were evaluated. The results show that the cyclic softening phenomenon exists under cyclic loading, and the steel has good load carrying capacity and cyclic energy dissipation capacity before and after corrosion, which can be used in corrosive environments and in structures with seismic requirements.

Keywords—high strength steel, cyclic principal structure, salt spray corrosion, mechanical properties

I. INTRODUCTION

The mechanical response of a structure under seismic action cannot be ignored, and the seismic action can be considered as a low circumferential cyclic loading of the structure. Many scholars have studied the cyclic mechanical properties of steel. Shi [1] *et al.* conducted cyclic loading tests on Q235B and Q345B structural steels commonly used in engineering and found that cyclic loading causes necking and fracture strains of specimens to advance. Shen [2] *et al.* conducted low circumferential cyclic tests on Q345GJ steel specimens and investigated the cyclic loading mechanical behavior of Q345GJ steel and found that the cyclic strengthening of steel is significantly affected by the loading history.

Dai [3] *et al.* conducted monotonic and cyclic loading tests on Q345 conventional steel and Q460 high-strength steel and analyzed the differences in mechanical properties of the two steels. The results showed that the cyclic

strengthening effect and the Bauschinger effect were more obvious for Q345 steel compared with Q460 high-strength steel; Q460 high-strength steel had better hysteretic properties and ductility than Q345 steel.

The cyclic mechanical properties of steel in corrosive environments are generally affected, and some studies have been conducted by scholars on this issue. Xu [4, 5] *et al.* conducted cyclic mechanical tests on Q235 steel plates after neutral salt spray corrosion to reveal the effect of corrosion damage on the cyclic mechanical properties of steel. Guo [6, 7] *et al.* conducted hysteresis tests on Q690 high-strength steel by indoor artificially accelerated simulated corrosion method, analyzed the macroscopic and microscopic morphology of Q690 high-strength steel under different corrosion levels, and revealed the influence of corrosion level on the mechanical properties of Q690 high-strength steel.

In general, with the development trend of domestic steel more high-strength, high-performance, for the new domestic high-strength steel cycle mechanical properties of research is very necessary. In addition, scholars are late to pay attention to the post-corrosion mechanical properties of steel, and most of the research on steel itself is focused on the corrosion resistance of conventional steel, and the research on the post-corrosion cyclic mechanical properties of high-strength steel is still relatively small. With the increase of application scenarios of high-strength steel in corrosive environments such as offshore platforms and tower structures, research on the corrosion resistance of new domestic high-strength steels is also urgently needed.

In this paper, the low circumferential cycle mechanical properties of the new Q960 high-strength steel from HISCO before and after corrosion are studied by means of tests, which are intended to lay the foundation for the promotion and application of domestic Q960 high-strength steel.

II. TEST PROCEDURE

A. Specimen Design

In this paper, 17 repeated cyclic loading specimens were obtained by full thickness sampling, and cyclic loading tests were carried out for seven of them under different loading regimes, corresponding to seven loading regimes, and salt spray corrosion tests and cyclic loading tests after corrosion were carried out for the other 10 cyclic specimens. The corrosion degree is set to five, each corrosion degree two specimens, corresponding to two loading systems. Specific specimen arrangement and the number of specimens as shown in Table I.

TABLE I. ARRANGEMENT AND QUANTITY OF TEST SPECIMENS

Test Type	Corrosion degree	Number of specimens	Total
Cycle test	C0	7	17
Cycle test	C1	2	
Cycle test	C2	2	
Cycle test	C3	2	
Cycle test	C4	2	
Cycle test	C5	2	

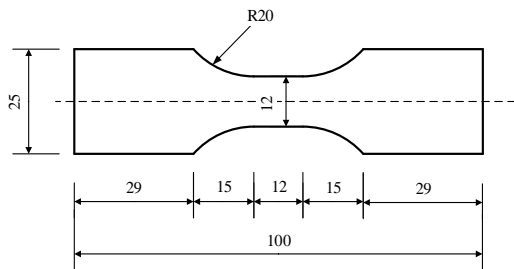


Fig. 1. Size of cyclic specimen(mm).

The design dimensions of the cyclic loaded specimens refer to the relevant requirements of Metallic materials—Fatigue testing—Axial-strain-controlled method (GB/T

26077-2021) [8], and the plate specimens are used, and the design dimensions are shown in Fig. 1. The numbering of cyclic loaded specimens adopts the form of C-X-Y, C is the initial letter of Cyclic, indicating cyclic loading; X indicates the loading system number, Y indicates the corrosion degree, C0 indicates no corrosion, C1 indicates corrosion for 10 days, C2 indicates corrosion for 20 days, C3 indicates corrosion for 30 days, C4 indicates corrosion for 40 days, and C5 indicates corrosion for 60 days.

B. Salt Spray Corrosion Test

This paper corrosion process with reference to Corrosion tests in artificial atmospheres—Salt spray tests (GBT 10125-2021) [9] in the copper accelerated acetic acid salt spray test (CASS test) content. Test five degrees of corrosion were corrosion 10 days, 20 days, 30 days, 40 days, 60 days, when the corrosion of the test piece to the corresponding time will be corroded test piece removed and the corrosion of the surface for water cleaning and acid cleaning rust removal. Cleaning process with reference to Corrosion of metals and alloys—Removal of corrosion products from corrosion test specimens (GBT 16545-2015) [10] to carry out.

C. Loading Equipment and System

The cyclic loading test was performed on the MTS 322 testing machine. Seven cyclic loading regimes were set up, as shown in Table II. There are seven cyclic loading regimes set up The loading regimes were named in the form of C-X, where C stands for cyclic loading and X stands for the loading regime number.

The deformation of the specimen during the monotonic stretching test was monitored by an electronic extensometer of model YYU-25/50, with a 50 mm scale, a maximum deformation of 25 mm and an accuracy of 0.5 grade.

TABLE II. CYCLIC LOADING PROTOCOL

Loading system number	Loading System
C-01	About the strain was loaded symmetrically at 0, the tension-compression strain level was maintained at 1%, and a total of 25 turns were loaded, first in tension and then in compression.
C-02	About the strain was loaded symmetrically at 0, the tension-compression strain level was maintained at 2%, and a total of 25 turns were loaded, first in tension and then in compression.
C-03	About the strain was loaded symmetrically at 0, the tension-compression strain level was maintained at 3%, and a total of 25 turns were loaded, first in tension and then in compression.
C-04	About the strain was loaded symmetrically at 0, the tensile and compressive strains were loaded in 0.25% increments from 0 in two turns per stage until the maximum compressive strain reached 3%, first in tension and then in compression.
C-05	About the strain was loaded symmetrically at 0, the initial tensile and compressive strains were maintained at the 3% level, and the tensile and compressive strains were reduced in 0.25% increments until they were reduced to 0. Each stage was loaded for two turns, first in tension and then in compression.
C-06	The compressive strain was kept at 0, and the tensile strain was increased in 0.25% increments starting from 0. Two turns were loaded at each level, and a total of 24 turns were loaded, with tensile first and compressive second.
C-07	The strain amplitude was kept constant at 4%, and the initial tensile and compressive strains were maintained at 2%, then the tensile strains were increased in 0.25% increments and the compressive strains were decreased in 0.25% increments, and a total of 24 turns were loaded, first in tension and then in compression.

III. ANALYSIS OF TEST RESULTS

A. Salt Spray Corrosion Test Results

Fig. 2 is the macroscopic corrosion morphology of high-strength steel specimens after corrosion. It can be seen that

the corrosion of the specimen surface is wrapped by a layer of iron oxide rust layer, the rust layer is brittle and easy to peel off, the longer the corrosion days the thicker the rust layer. Corrosion 10 days after the test specimen rust layer close to the surface of the test specimen, due to corrosion

has not reached uniform, the surface of the test specimen shows a patchy form; corrosion 20 days later, corrosion tends to uniform, rust layer on the surface of the test specimen began to slightly raised; corrosion 30 days and corrosion 40 days later, the surface of the test specimen rust layer began to bulge, and uniformly wrapped test specimen; corrosion 60 days after the surface of the test specimen rust layer color deepened, and produce flaking.

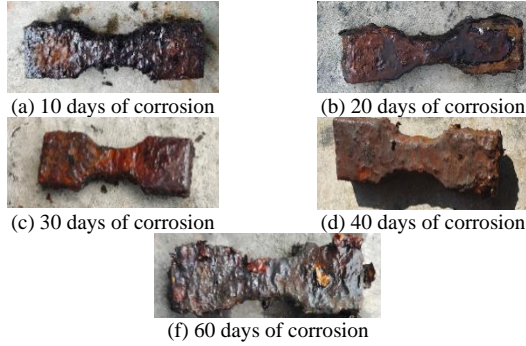


Fig. 2. Macroscopic morphology of corrosion specimens.

After pickling the corroded specimen, the microscopic corrosion morphology of the corroded specimen of high-strength steel can be photographed, as shown in Fig. 3. It can be seen that after 10 days of corrosion, the specimen local location of the obvious corrosion pits; corrosion 20 days later, the corrosion pits significantly reduced, to corrosion 30 days, has basically invisible corrosion pits, the specimen surface began to become flat; to corrosion 40 days, 60 days, the specimen surface has been very flat. This shows that the corrosion of the initial specimen to pitting corrosion is the main, and with the increase in the number of days of corrosion, the specimen to uniform corrosion is the main. The longer the number of days of corrosion, the flatter the surface of the specimen, the longer the corrosion time the more uniform corrosion.

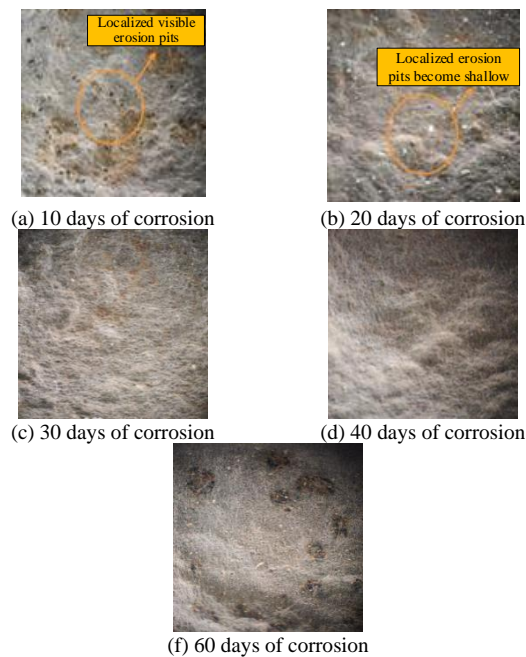


Fig. 3. Microstructure of corrosion specimens.

Material quality loss can be characterized using the mass loss rate, the mass loss rate that the test piece in the corrosion process loss of mass as a percentage of the mass before corrosion. Its calculation formula is shown in Eq. (1).

$$\gamma = \frac{M_0 - M_1}{M_0} \times 100\% \quad (1)$$

where, γ the mass loss rate of the specimen, M_0 represents the mass of the specimen before corrosion, M_1 represents the mass of the specimen after corrosion.

The quality loss rate of the specimens under different corrosion days of high strength steel were averaged, and the average quality loss rate of high strength steel specimens can be obtained in relation to the number of days of corrosion, as shown in Table III. It can be seen that the specimen quality loss rate and corrosion time is approximately linear relationship, the linear fit results are shown in Fig. 4.

TABLE III. AVERAGE MASS LOSS RATE

Number of days of corrosion	0	10	20	30	40	60
Average quality loss rate of base material γ (%)	0	3.12	4.52	5.65	6.90	11.07

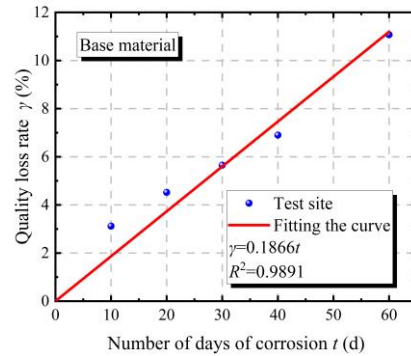
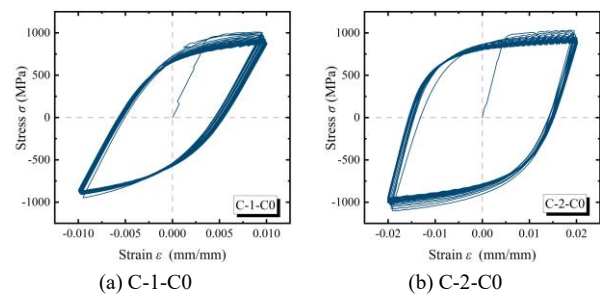


Fig. 4. Average mass loss rate - corrosion days curve.

B. Cyclic Loading Test Results

The deformation of the specimens during the cyclic loading test was monitored by an elongometer with an 8 mm scale. During the cyclic test, no buckling occurred in each specimen. The cyclic stress-strain curves of the high-strength steel specimens under various loading regimes are shown in Fig. 5.



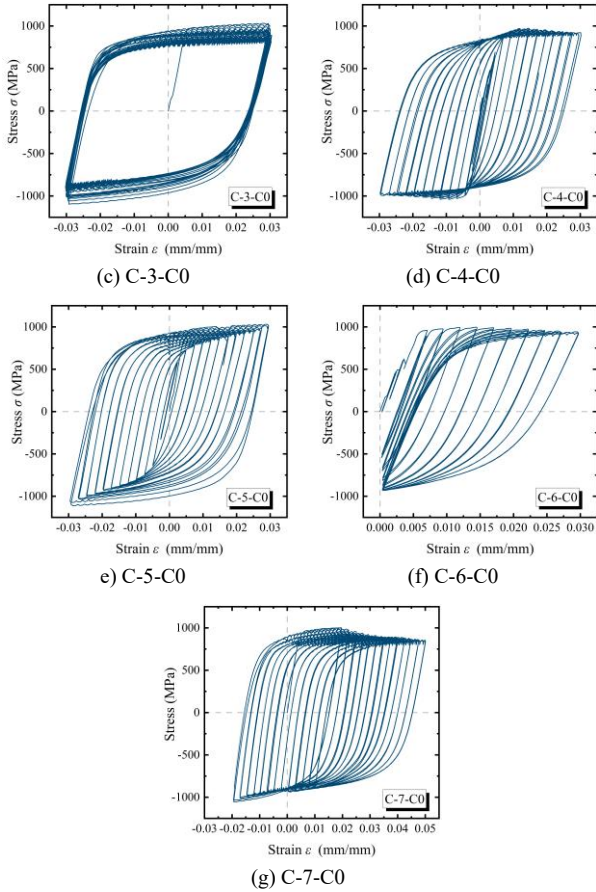


Fig. 5. Cyclic stress-strain curves of base metal specimens.

The cyclic stress-strain curves of the specimens are all in a relatively full shuttle shape with good hysteresis properties. The Bauschinger effect of the material is relatively obvious, and the obvious cyclic softening and obvious strain hardening characteristics occur during the cycling process. From Fig. 5(g), it can be seen that the hysteresis loop area decreases with the increase in the number of cycle turns when the strain amplitude is kept constant, indicating that the work done by the steel in the cycle decreases with the increase in the number of cycle turns.

The cyclic stress-strain curves of the specimens after corrosion are shown in Fig. 6. Overall, the cyclic stress-strain curves of the post-corrosion specimens are relatively full shuttle-shaped, compared with the shape before corrosion, there is no significant difference, the post-corrosion specimens still have the Bauschinger effect, cyclic softening, strain hardening characteristics.

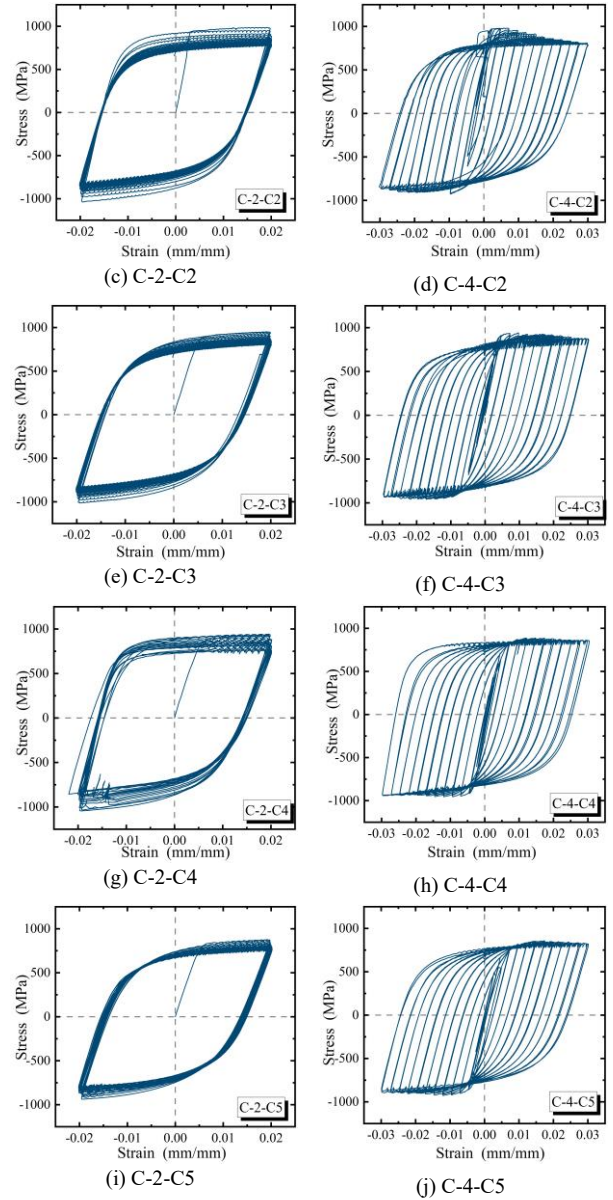
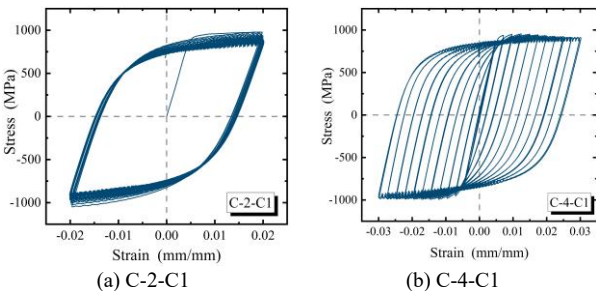


Fig. 6. Cyclic stress-strain curves of specimens after corrosion.

The relationship between the nominal yield stress of Q960 steel specimens and the number of days of corrosion is shown in Table IV. As can be seen from the graph, the nominal yield stress of the specimen is high at 20 days of corrosion, which is caused by stalling in the early stage of loading, and this point is excluded as an anomaly in the data fitting. From the fitting results, the nominal yield stress of the high-strength steel specimen decreases with the number of days of corrosion is basically linear, and the nominal yield stress of the high-strength steel specimen decreases by about 14% after 60 days of corrosion. Specimen nominal yield stress σ_y with the number of days of corrosion t and mass loss rate γ change relationship as shown in Eq. (2), Eq. (3) and Fig. 7.

$$\sigma_y = -2.22t + 970.49 \quad (2)$$

$$\sigma_y = -11.90\gamma + 970.49 \quad (3)$$

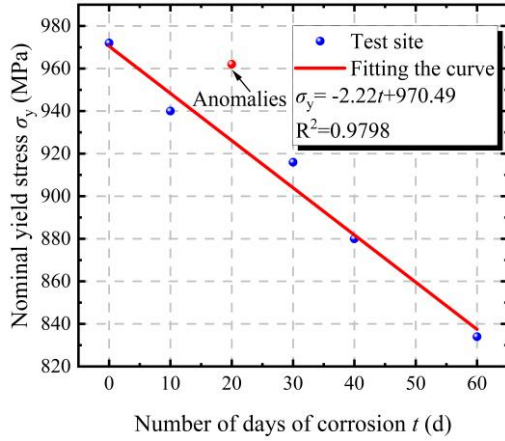


Fig. 7. Relationship between nominal yield stress and corrosion days.

TABLE IV. RELATIONSHIP BETWEEN NOMINAL YIELD STRESS AND CORROSION DAYS

Number of days of corrosion	0	10	20	30	40	60
Nominal yield stress	973	940	962	916	880	834
Yield stress reduction rate (%)	0	3.39	1.13	5.86	9.56	14.29

C. Skeleton Curve

The skeleton curve of the material is an important indicator of the cyclic mechanical properties of the material. The skeleton curve of the material can be obtained by connecting the extreme value points of the load in the same direction of each hysteresis circle of the material hysteresis curve.

Fig. 8 shows the comparison of Q960 high-strength steel skeleton curves under different corrosion days, it can be seen that with the increase of corrosion days, the bearing capacity of the specimens are gradually decreased. In order to visually reflect the change of skeleton curve stress with the corrosion degree, Fig. 9 shows the relationship between the skeleton curve stress and the corrosion days of the specimen when the strain is 1.5%. It can be seen that at this time, high strength steel skeleton curve stress with the number of days of corrosion is linearly decreasing.

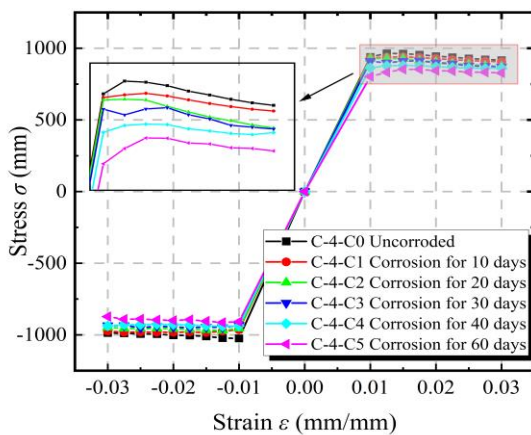


Fig. 8. Comparison of skeleton curves under different corrosion days.

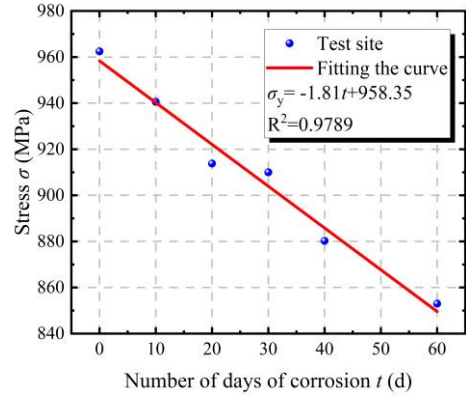


Fig. 9. Relationship between skeleton curve stress and corrosion days.

D. Energy Consumption Capacity

The energy dissipation capacity of a material under cyclic loading can reflect its seismic performance, and in order to quantify the energy dissipation capacity of a material, the concept of energy dissipation factor [11] can be introduced. The energy dissipation factor (also called energy dissipation factor) EDI is an important indicator to evaluate the energy dissipation capacity of a material and is calculated as shown in Eq. (4).

$$E_c = \frac{S_{ABC} + S_{CDA}}{S_{OBE} + S_{OFD}} \quad (4)$$

The $S_{ABC} + S_{CDA}$ in the numerator is equal to the area enclosed by the hysteresis loop formed during each cycle of the hysteresis curve, and the $S_{OBE} + S_{OFD}$ in the denominator is equal to the triangular area enclosed by the origin of the coordinate, the extreme point of the hysteresis loop in the direction of tension (pressure) and its projection on the horizontal coordinate axis. The larger the EDI value of the material, the fuller the hysteresis loop and the stronger the energy dissipation capacity of the material, as shown in Fig. 10.

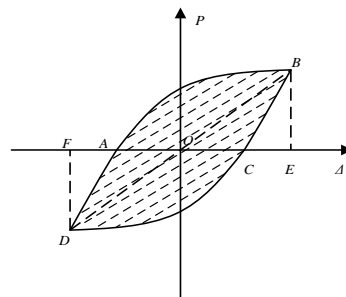


Fig. 10. Schematic diagram of energy dissipation coefficient calculation.

Fig. 11 shows the comparison of energy dissipation coefficients of Q960 high-strength steel specimens at the first and second cycles of each stage during cyclic loading. It can be seen from the figure that the value of the energy dissipation coefficient of the specimen at the second cycle is almost equal to the value of the energy dissipation coefficient at the first cycle. The larger the strain amplitude

is, the larger the value of the energy dissipation coefficient is, and with the increase of the strain amplitude, the growth rate of the energy dissipation coefficient gradually slows down and finally stabilizes.

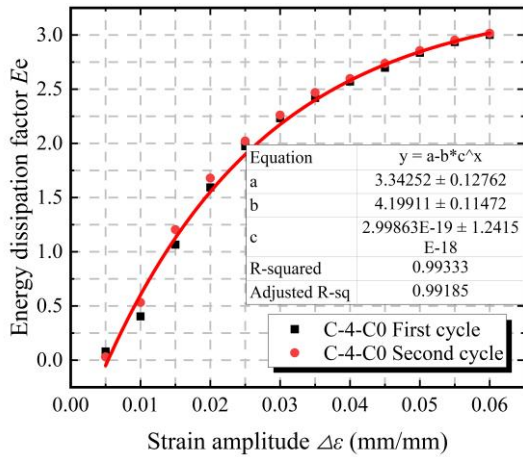


Fig. 11. Relationship between energy dissipation coefficient and cycle number at each stage.

The ultimate energy dissipation capacity of high tensile steel can be predicted by fitting the energy dissipation coefficient-strain amplitude curve. The graph shows that the ultimate value of energy dissipation coefficient of Q960 high tensile steel can be above 3.0, which indicates that high tensile steel can dissipate energy well under large strain amplitude.

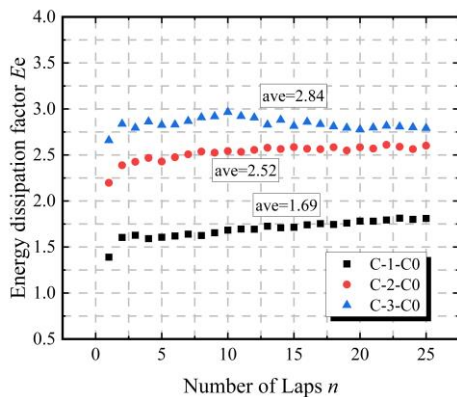


Fig. 12. Constant amplitude load energy dissipation coefficient under different strain amplitude.

Fig. 12 and Table V lists the average values of energy dissipation coefficients at different strain amplitudes under variable amplitude loading regime 4 for the specimens under constant amplitude loading regimes 1, 2 and 3 (the average values have been marked in the figure). It can be seen that the energy dissipation coefficient of constant amplitude loading is larger than that of variable amplitude

loading under the same strain amplitude, which indicates that the energy dissipation coefficient grows more slowly when the loading strain is smaller in the first period. It can be seen that the loading history has an effect on the energy dissipation capacity of high-strength steel.

Fig. 13 shows the cyclic energy dissipation coefficient of the corroded Q960 high-strength steel specimens under different degrees of corrosion. On the whole, the energy dissipation coefficient of high-strength steel tends to the same stable value of 2.5 or so as the number of cycles increases. This indicates that the energy dissipation capacity of high-strength steel specimens with normal amplitude loading is only related to the material properties of the steel itself, and is not related to the degree of corrosion of the steel, even if the long time in a corrosive environment, high-strength steel can maintain a good energy dissipation capacity. Fig. 14 shows the cyclic energy dissipation coefficient of Q960 high-strength steel specimens loaded with variable amplitude under different degrees of corrosion. It can be seen that the energy dissipation coefficient changes in the same pattern as before corrosion.

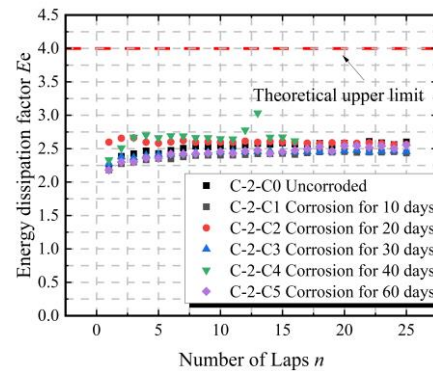


Fig. 13. Relationship between energy dissipation coefficient and corrosion degree.

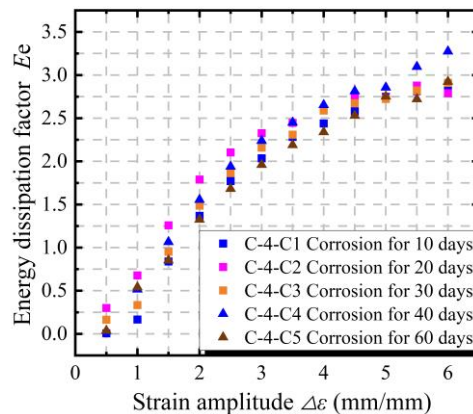


Fig. 14. Relationship between energy dissipation coefficient and strain amplitude.

TABLE V. AVERAGE ENERGY DISSIPATION COEFFICIENT UNDER DIFFERENT STRAIN AMPLITUDE

$\Delta\varepsilon$ (%)	0.5	1	1.5	2	2.5	3	3.5	4	4.5	5	5.5	6
Materials												
Q960 steel	0.06	0.47	1.13	1.64	2.00	2.25	2.44	2.58	2.72	2.85	2.94	3.01

IV. CONCLUSION

(1) During cyclic loading, the Q960 steel developed by HSC has more obvious Bauschinger effect, strain hardening and cyclic softening phenomena, and its cyclic stress level and energy dissipation capacity are related to cyclic loading history.

(2) In the corrosion process Q960 high strength steel predominantly pitting corrosion in the early stage, the late

(3) Transformation to homogeneous corrosion is dominant, corrosion after the quality loss rate with the increase in the number of days of corrosion is a linear increase.

(4) Corrosion will reduce the ductility, bearing capacity and hysteresis energy of high-strength steel specimens, but will not affect the energy dissipation coefficient of high-strength steel specimens. The hysteresis curve characteristics of the corroded high-strength steel specimens are similar to those of the specimens before corrosion, indicating that the material still has good cyclic mechanical properties after corrosion.

CONFLICT OF INTEREST

The authors declare no conflict of interest.

AUTHOR CONTRIBUTIONS

Sikai Liu wrote the original draft of the paper; Shidong Nie provided conceptualization and methodology; Zhenye Chen reviewed and edited the manuscript; Cheng Ma and Jin Pan provided materials relevant data; all authors had approved the final version.

FUNDING

Fund Projects: Basic research on the design and application of 690 MPa new high-performance structural steel for buildings (H20200688), The Project of Higher Education Discipline Innovation Introduction Program (B18062).

ACKNOWLEDGMENT

The authors would like to acknowledge the financial supports given through the Research, Design and

Application Project of Structural High-performance Steel of 690 MPa (Grant Project No. H20200688) and 111 Project (Grant No. B18062).

REFERENCES

- [1] Y. J. Shi, M. Wang, and Y. Q. Wang, "Experimental and constitutive model study of structural steel under cyclic loading," *Journal of Constructional Steel Research*, vol. 8, pp. 1185–1197, August 2011.
- [2] L. Shen, M. Ding, C. Feng, B. Yang, M. Elchalakani, and L. J. Song, "Experimental study on the cumulative damage constitutive model of high-performance steel Q345GJ under cyclic loading," *Journal of Constructional Steel Research*, vol. 181, June 2021.
- [3] G. X. Dai, F. Wang, G. Shi, Y. Q. Wang, and Y. J. Shi, "Comparison of monotonic and cyclic performances of structural steel Q345 and Q460," *Industrial Construction*, 1: 13–17, June 2012.
- [4] S. H. Xu, H. Wang, and L. Su, "Degradation law of mechanical properties of Q235 steel plate in neutral salt spray corrosion environment," *Materials for Mechanical Engineering*, vol. 5, pp. 86–91, March 2015.
- [5] S. H. Xu, C. G. Qin, Z. X. Zhang, and Y. D. Wang, "Experimental study on hysteretic behavior of corrosion steel in the neutral salt spray," *Journal of Harbin Institute of Technology*, vol. 11, pp. 183–188, October 2015.
- [6] H. C. Guo, T. Y. Li, D. F. Wang, D. X. Gao, and X. L. Li, "Hysteretic properties of corroded high strength steel in marine environment," *Journal of Building Materials*, vol. 4, pp. 781–787, February 2020.
- [7] H. C. Guo, S. J. Zhang, T. X. Li, D. W. Zhang, Y. L. Li, and Y. H. Liu, "Research on mechanical property degradation of corroded Q690 high-strength steel in the marine environment," *Industrial Construction*, vol. 8, pp. 184–189, December 2020.
- [8] Metallic materials—Fatigue testing—Axial-strain-controlled method, GB/T 26077-2021.
- [9] Corrosion tests in artificial atmospheres—Salt spray tests, GB/T 10125-2021.
- [10] Corrosion of metals and alloys—Removal of corrosion products from corrosion test specimens, GB/T 16545-2015.
- [11] N. Masayoshi, "Strain-hardening behavior of shear panels made of low-yield steel. I: Test," *Journal of Structural Engineering*, vol. 12, pp. 1742–1749, December 1995.

Copyright © 2024 by the authors. This is an open access article distributed under the Creative Commons Attribution License (CC BY-NC-ND 4.0), which permits use, distribution and reproduction in any medium, provided that the article is properly cited, the use is non-commercial and no modifications or adaptations are made.